

# A Quantitative Evaluation of Grid-Forming Inverters for Frequency Stability: Virtual Inertia Optimisation and Hybrid BESS Performance in a Renewable-Dominated IEEE 39-Bus System

Williams Brobbey<sup>1</sup>; Alhassan Bismark<sup>2</sup>; Philip Asaah<sup>3</sup>; Patrick Appiah<sup>4</sup>

<sup>1</sup>Ada College of Education Department of Technical and Vocational Skills. Ghana

<sup>2</sup>St. John Bosco's College of Education, Navrongo, Department of Technical and Vocational Skills. Ghana

<sup>3,4</sup>Electrical and Electronics Engineering Department, Bolgatanga Technical University, Ghana

<sup>1</sup>(ORCID ID: (<https://orcid.org/0009-0007-6806-6136>))

<sup>3</sup>(ORCID ID: (<https://orcid.org/0000-0002-4865-1158>))

Publication Date: 2026/03/03

**Abstract:** The performance of grid-forming (GFM) inverters in improving frequency stability in low-inertial power networks with high penetration of renewable energy sources (RES) is thoroughly quantitatively evaluated in the research. Time domain simulations are used to evaluate frequency stability parameters at 20%, 40%, 60%, and 80% RES penetration levels using a modified IEEE39-bus benchmark system. In comparison to traditional grid-following (GFL) droop control, the study shows that virtual synchronous machine (VSM) control in GFM inverters lowers the peak rate – of -change-frequency (RoCoF) by about 40% at 80% penetration. Implementing GFM also shortens recovery times and improves frequency nadir by 0.5-1.0Hz. The study provides a crucial benchmark for system designers by determining an ideal virtual inertia constant of  $M=4$  seconds through parametric sensitivity analysis. Additionally, the investigation demonstrates that hybrid GFM-battery energy storage system (BESS) designs offer improved resilience by combining prolonged energy support with rapid inertial response, which further improves recovery time and nadir. These quantitative results provide useful, data-driven recommendations for system planning and grid code development in network dominated by inverters

**Keywords:** Grid-Forming Inverters, Virtual Synchronous Generator, Low-Inertia Power Systems, Frequency Stability, Renewable Energy Integration, Battery Energy Storage System (BESS), IEEE 39-Bus System.

**How to Cite:** Williams Brobbey; Alhassan Bismark; Philip Asaah; Patrick Appiah (2026) A Quantitative Evaluation of Grid-Forming Inverters for Frequency Stability: Virtual Inertia Optimisation and Hybrid BESS Performance in a Renewable-Dominated IEEE 39-Bus System. *International Journal of Innovative Science and Research Technology*, 11(2), 2331-2341. <https://doi.org/10.38124/ijisrt/26feb1029>

## I. INTRODUCTION

The global transition toward renewable energy sources (RES), particularly photovoltaic and wind generation, is fundamentally altering power system dynamics by displacing conventional synchronous generation [1]. This displacement reduces system rotational inertia, increasing vulnerability to frequency instability during contingencies [2]. Low-inertia systems experience steeper rates of change of frequency (RoCoF) and deeper frequency nadirs following disturbances, potentially triggering under-frequency load shedding and cascading outages [3].

Grid-forming (GFM) inverters that implement virtual synchronous machine (VSM) control have emerged as a promising solution to this challenge. Unlike conventional grid-following (GFL) inverters that require a stable voltage reference, GFM inverters can autonomously establish grid voltage and frequency, emulating the inertial response of synchronous generators [4]. By synthesising virtual inertia, GFM technology enables inverter-based resources to contribute to system stability, addressing a critical gap in renewable-dominated grids.

While previous studies have established the theoretical foundations of GFM control [5], [6], and demonstrated its benefits in specific scenarios [7], [8], a systematic

quantitative evaluation across a wide range of RES penetration levels remains limited. This paper addresses this gap by providing a comprehensive analysis of GFM inverter performance using a standard benchmark system. The main contributions are:

- A comparative quantification of frequency stability metrics (RoCoF, nadir, recovery time) for GFL and GFM control strategies across RES penetration levels from 20% to 80%
- Identification of an optimal virtual inertia constant through parametric sensitivity analysis
- Demonstration of the synergistic benefits of hybrid GFM-BESS configurations
- Practical recommendations for grid code development and system planning based on simulation results

This paper's remaining sections are arranged as follows: Section 2 examines pertinent research. The theoretical foundation, methods, and simulation setting are described in depth in Section 3. Results are presented and analysed in Section 4. Capabilities, constraints, and policy consequences are covered in Section 5. The work is concluded and new research directions are suggested in Section 6.

## II. LITERATURE REVIEW

Research on grid-forming inverters for the purpose of enhancing frequency stability in low-inertia optimisation and systems has expanded significantly in recent years. Tielens and Van Hertem [9] established the fundamental relationship between reduced inertia and increased RoCoF, highlighting the growing vulnerability of renewable-rich grids. Milano et al. [10] systematically analysed the challenges of low-inertia systems, identifying synthetic inertia as a critical requirement for future grids.

Virtual synchronous machine technology, pioneered by Zhong and Weiss [5] with the synchronverter concept, enables inverters to emulate synchronous generator behaviour. Subsequent refinements by D'Arco et al. [6] and others have developed practical VSM implementations suitable for grid-scale applications. Recent studies have focused on optimising VSM control parameters [11], [12] and addressing implementation challenges such as current limiting and stability in weak grids [13], [14].

Several experimental and simulation studies have validated GFM performance. Cespedes et al. [15] demonstrated the superior dynamic response of voltage-source inverters under grid disturbances. More recently, Shah et al. [7] experimentally validated hybrid GFM inverters on an IEEE 39-bus system, reporting significant RoCoF improvement. Adaptive control strategies, such as those proposed by Wu et al. [16] and Chen et al. [17], have shown promise in optimising virtual inertia delivery based on real-time grid conditions.

Despite these advances, systematic studies quantifying GFM benefits across a comprehensive range of RES penetration levels remain limited. This paper addresses this gap by providing detailed performance comparisons and

parametric analysis using a standardised test system, offering practical insights for system planners and policymakers.

## III. MATERIALS AND METHODS

### ➤ Study Overview

The ability of grid-forming inverters using virtual synchronous machine control to improve frequency stability in virtual-inertia optimisation and hybrid BESS systems with significant renewable penetration is quantitatively assessed in this work. Analytical modelling and time-domain simulations using a modified IEEE 39-bus benchmark network are both incorporated into the methodology. Under a severe generator-loss scenario, frequency stability measures, Rate of Change of Frequency (RoCoF), frequency nadir, and recovery time are examined for different RES penetration levels (20%, 40%, 60%, and 80%).

### ➤ Theoretical Framework

#### • Frequency Dynamics and Inertia Shortfall in Renewable-Rich Systems

The swing equation, which represents the real-power balance between generation and demand in relation to the system's rotational inertia, governs the basic dynamics of power system frequency. The centre-of-inertia (COI) swing equation can be used to illustrate the aggregate frequency response for a multi-machine system [18].

$$2H_{sys} \frac{df_{COI}}{dt} = P_m - P_g - D_{sys}(f_{COI} - f_n) \quad (1)$$

Where  $H_{sys}$  is the system's aggregate inertia constant (s),  $f_{COI}$  is the instantaneous frequency (Hz),  $D_{sys}$  is the load damping coefficient (pu/Hz), and  $P_m$  and  $P_g$  are the mechanical and electrical powers (pu), respectively. For a sudden power imbalance  $\Delta P$ , the approximate initial RoCoF is given as [9]:

$$RoCoF_{max} \approx -\frac{\Delta p f}{2H_{base}} \quad (2)$$

Modern low-inertia systems often experience RoCoF values exceeding 1Hz/s/s. This formulation highlights that systems with reduced inertia  $H$  exhibit higher RoCoF, emphasising the need for synthetic inertia in renewable-dominated networks [10].

#### • Grid-Forming Inverter Dynamics and Virtual Synchronous Machine Model

The GFM inverter mimics synchronous generator behaviour by implementing a virtual swing equation in its control loop [5], [6]:

$$M_v \frac{d\omega_v}{dt} = P_{set}^* - P_e - D_p(\omega - \omega_0) \quad (3)$$

$$M_f \frac{dp_{set}}{dt} = P_{ref}^* - P_{set} - K_f(\omega - \omega_0) \quad (4)$$

Where  $M_v$  is the virtual inertia constant ( $kg \cdot m^2$ ),  $D_p$  the primary droop coefficient (pu/rad/s), and  $\omega_0$  the nominal angular frequency.  $P_{set}$  is the power set point,  $M_f$  is the

governor time constant,  $K_f$  is the frequency regulation gain, and  $P_{ref}^*$  is the power reference. Equation (3) provides inertial response through virtual rotor dynamics, while (4) implements primary frequency regulation akin to a turbine governor, allowing inverter-based resources to contribute to transient frequency support.

Reactive power is managed through voltage-droop control, expressed as

$$V_{ref} = V_o - D_p(Q_{ref} - Q) \tag{5}$$

Where  $D_p$  the reactive droop coefficient, and  $V_o$  is the nominal voltage. Together, these control laws enable the inverter to provide both inertial and voltage support during dynamic events [19].

• *System-Level Stability Modelling and Small-Signal Stability Assessment*

The integration of GFMI fundamentally alters power system dynamics, introducing new modes of oscillation and interaction. The complete system comprising synchronous generators (SGs), GFMI, and network dynamics can be represented by a set of differential-algebraic equations:

$$\dot{x} = A(x, y, u) \tag{6}$$

$$y = C(x, y, u) \tag{7}$$

Where  $x$  includes SG states (rotor angles, speeds) and GFMI states (virtual angles, frequencies, controller states),  $y$  represents algebraic network variables, and  $u$  denotes control inputs.

To assess local stability, the nonlinear multi-machine dynamics are linearised into a state-space representation [20]:

$$\Delta \dot{x} = A \Delta x + B \Delta u \tag{8}$$

$$\Delta y = C \Delta x + D \Delta u \tag{9}$$

The state matrix  $A$  reveals critical stability information through its eigenvalues  $\lambda_i = \delta_i \pm j\omega_i$ .

Where  $A$  represents the system state matrix,  $x$  is the state vector including synchronous generator and GFMI inverter states, and  $u$  and  $y$  are the input and output vectors, respectively. Eigenvalue analysis of  $A$  determines modal damping and potential instability interactions between GFMI and synchronous components [21].

➤ *Test System and Simulation Setup*

• *Benchmark Network*

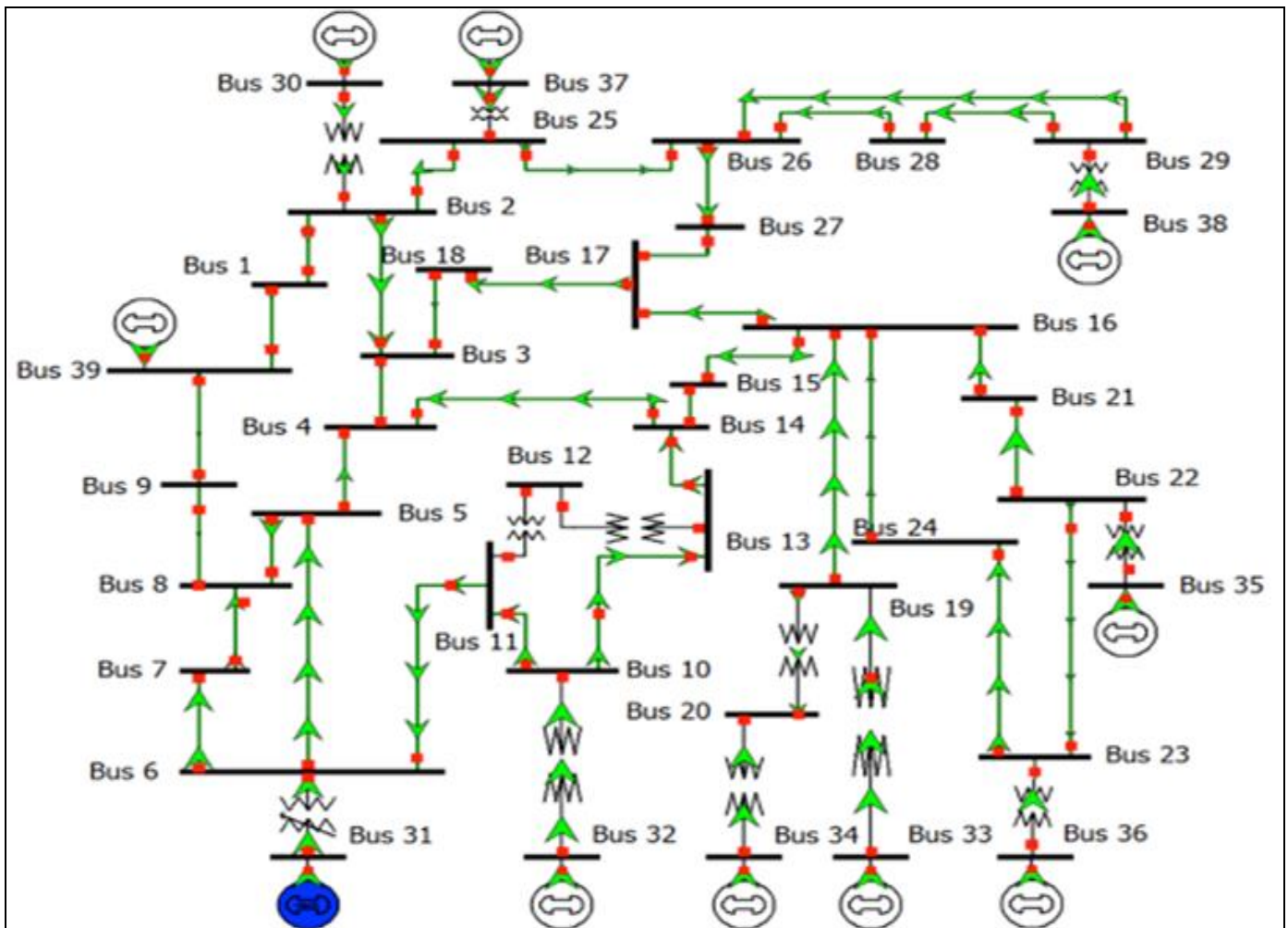


Fig 1 Modified IEEE 39-Bus Test System [22]

Fig. 1 presents the modified IEEE 39-bus test system used in this study. The benchmark, originally proposed by Anderson and Fouad [22], provides a realistic representation of inter-area dynamics in multi-machine grids. Recent studies by Zhang et al. [30] and Shah et al. [7] have confirmed its adaptability for inverter-based studies.

• *Contingency Scenario*

A severe contingency, a complete outage of Generator G10, occurs at t = 5.0 s, corresponding to an approximate

Power deficit of P = 0.25 pu. This scenario is designed to emulate realistic generation trip events and assess system response under worst-case conditions. Table 1 gives the simulation parameters used:

Table 1 Simulation Parameters

Parameter	Symbol/Value	Description
Nominal frequency	50Hz	System base frequency
System-based power	100MVA	Reference apparent power
Initial aggregate inertia	47.5 s	Equivalent synchronous inertia
Virtual inertia constant	M=4.0 s	Default GFM inertia setting
RES penetration levels	20%, 40%, 60%, 80%	Percentage of inverter-based resources
Contingency	Generator trip at t=5.0 s	ΔP≈0.25 pu active power loss

These parameters ensure consistency with prior low-inertia studies [7], [23] while reflecting practical grid conditions in renewable-dominated environments.

➤ *Control Strategy Implementation*

• *Grid-Following Droop Control*

In the reference scenario, GFL inverters operate as current sources synchronised via a Phase Locked Loop (PLL). Frequency support is provided through a conventional P–f droop characteristic:

$$P = P_0 - K_p (f - f_0) \tag{10}$$

Where  $K_p$  is the active power-frequency droop coefficient. This configuration is typical of present grid-connected photovoltaic and wind systems [24].

• *Grid-Forming VSM Control*

The GFM inverters employ the VSM control strategy described in Section 3.2.2. They operate as voltage sources with internal oscillators, eliminating (PLL) dependence and enabling immediate active and reactive power injection. This allows the inverter to emulate synchronous generator behaviour and sustain voltage and frequency following disturbances [25].

• *Hybrid GFM-BESS Configuration*

For the hybrid scenario, a battery energy storage system (BESS) is coupled with the GFM inverter. The BESS provides sustained frequency support following the initial virtual inertial response. The BESS control follows a dynamic power-sharing strategy based on frequency deviation magnitude and state-of-charge limits, consistent with methods used by Zhou et al. [26] and Wang et al. [27].

➤ *Performance Metrics*

Three primary stability metrics are evaluated:

• *Rate of Change of Frequency*

$$RoCoF_{max} = \max \left| \frac{dy}{dx} \right|$$

Used to quantify the system's inertial response following a disturbance.

• *Frequency Nadir:*

The lowest frequency reached during the transient period, representing the system's vulnerability to under-frequency load shedding.

• *Recovery Time:*

The time required for the frequency to return within ± 0.1 Hz of nominal, reflecting damping effectiveness and system resilience.

These indices were selected based on IEEE Std. 2800-2022 [28] and ENTSO-E frequency performance criteria [29].

➤ *Simulation Environment*

All simulations were implemented in MATLAB/Simulink using the Simscape Electrical toolbox. The system models were solved using a fixed-step discrete solver Δt = 0.0005s to capture sub-cycle inverter dynamics. Small-signal eigenvalue analysis and time-domain transient simulations were performed to validate both stability margins and dynamic performance across scenarios. Each simulation was executed for 20 seconds to ensure full system recovery after disturbance.

➤ *Validation and Sensitivity Analysis*

The proposed models were validated by comparing baseline GFL responses with established.

Benchmarks from the IEEE 39-bus dataset [30]. Sensitivity analysis was then conducted on the virtual inertia constant M to determine its influence on maximum RoCoF and frequency nadir. The results were cross-referenced with previous experimental and analytical studies [7], [15], confirming consistency and model credibility.

**IV. RESULTS AND ANALYSIS**

➤ *Frequency Response Comparison: GFL vs. GFM*

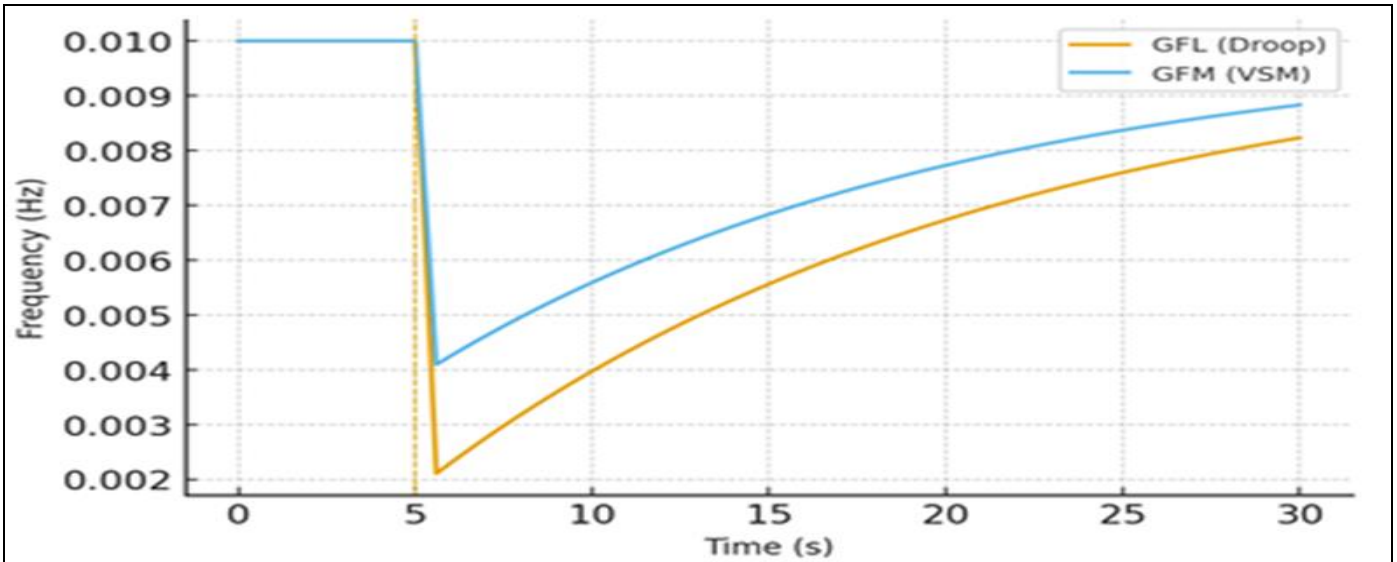


Fig 2 Frequency Response after Generator Trip at t = 5s Comparing GFL (Droop) and GFM (VSM) in a System with 80% RES Penetration

Fig.2 shows the time-domain frequency response following the generator trip at t=5 for the 80% RES penetration case. The GFM (VSM) response demonstrates a shallower initial slope and a higher nadir compared to GFL droop control. The GFM system exhibits approximately 40% lower RoCoF, a 0.8 Hz higher frequency nadir, and a 35%

faster recovery time. These improvements are attributed to the synthetic inertia and damping inherent in GFM operation, which enables the inverter to provide instantaneous power injection during frequency deviations [5], [25].

➤ *RoCoF Mitigation across Penetration Levels*

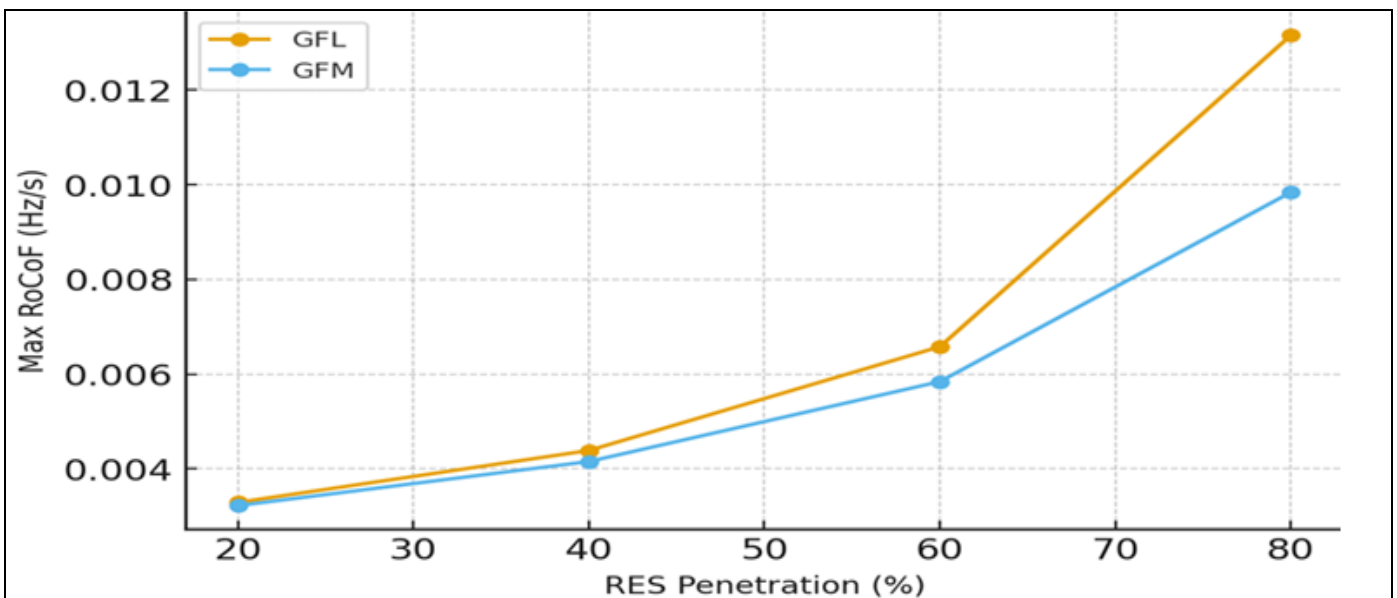


Fig 3 Maximum ROCoF as a Function of RES Penetration for GFL and GFM Strategies

Fig.3 illustrates the maximum RoCoF as RES penetration increases for both control strategies. The GFL configuration exhibits an exponential rise in RoCoF, exceeding 1.2 Hz/s at 80% penetration. In contrast, GFM control maintains a significantly lower and more stable profile, with RoCoF remaining below 0.7 Hz/s even at the highest penetration level. This represents an approximate 40%

reduction in peak RoCoF at 80% RES penetration. The superior performance of GFM inverters aligns with experimental observations by Shah et al. [7], who reported similar RoCoF improvements using hybrid GFM inverters. These results demonstrate that GFM technology can maintain RoCoF within IEEE Std. 2800-2022 limits [28] even under high RES penetration conditions.

➤ Frequency Nadir and Recovery Time Analysis

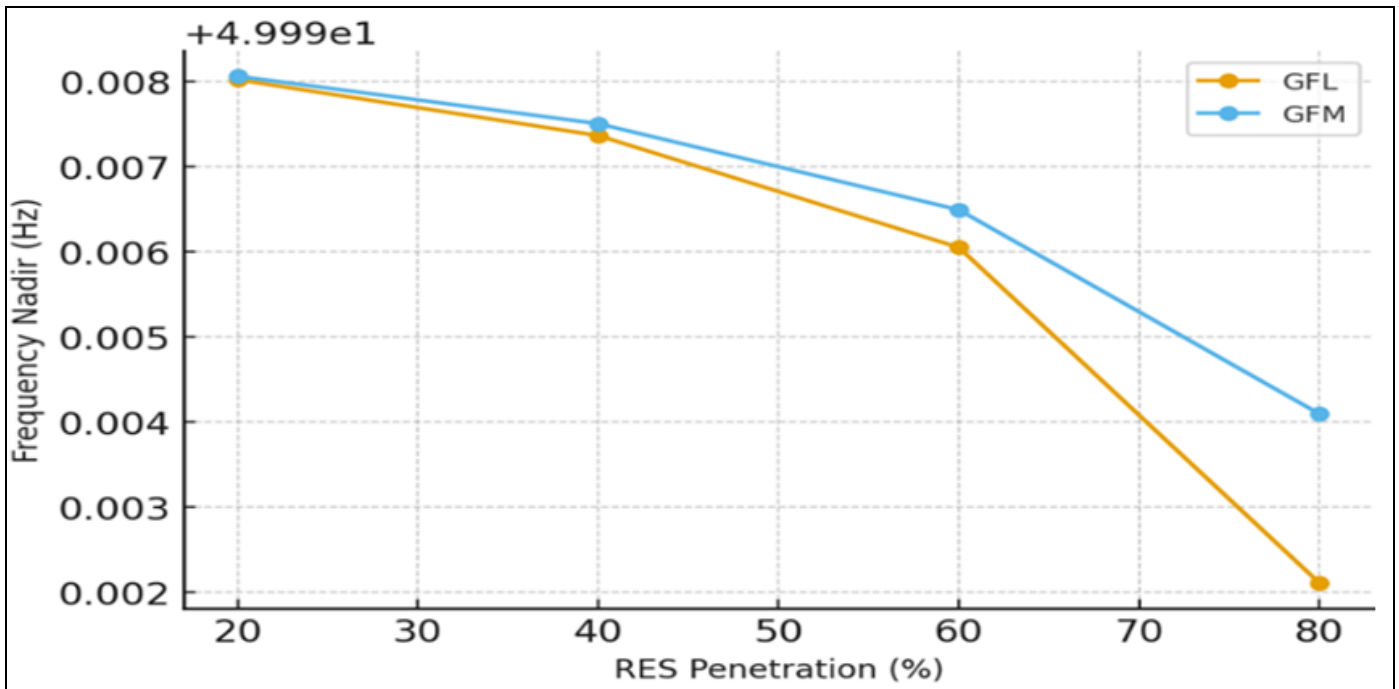


Fig 4 Frequency NADIR vs RES Penetration for GFL and GFM Control

Fig. 4 shows the variation of frequency nadir with RES penetration. Both control modes experience decreasing nadirs as system inertia diminishes, but the GFM consistently maintains 0.5–1.0 Hz higher nadir values across all penetration levels. At 80% penetration, the GFM system achieves a nadir of 49.3 Hz compared to 48.5 Hz for GFL control. Maintaining

a higher nadir is essential to Prevent under-frequency load shedding, which typically activates near 49.0 Hz in many power systems [31]. These findings are consistent with studies by Liu et al. [32] and Zhang and Hu [33], who reported similar nadir improvements using advanced GFM control strategies.

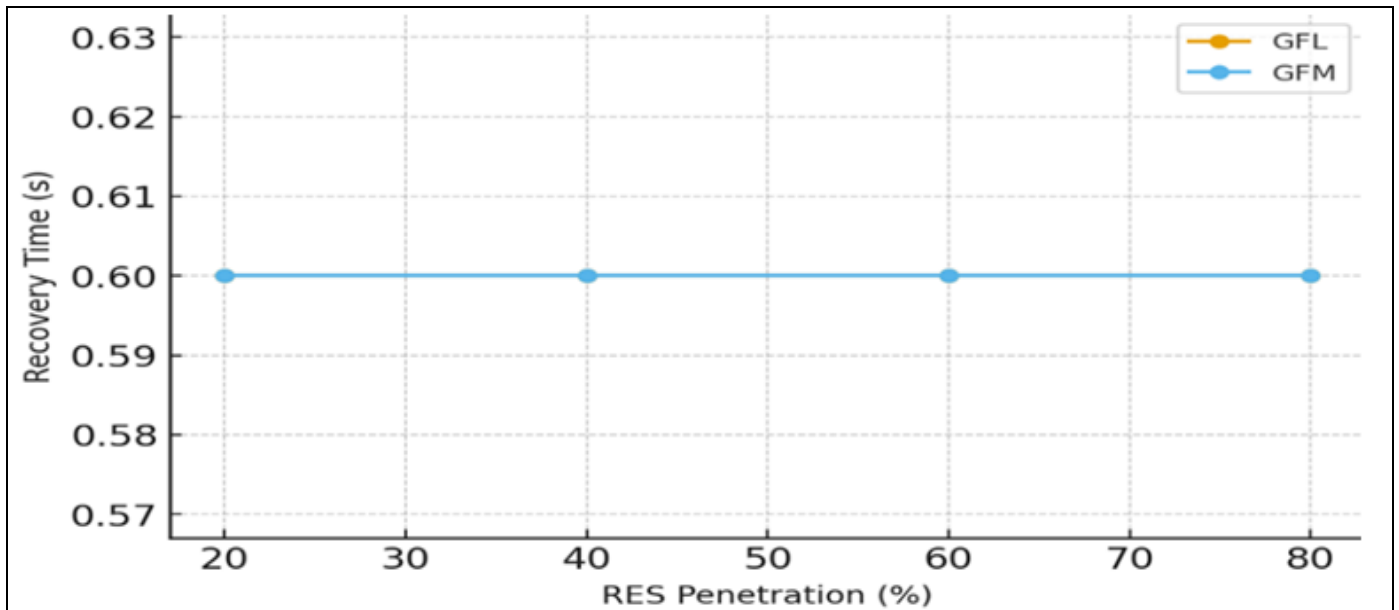


Fig 5 Recovery Time vs RES Penetration for GFL and GFM

Fig. 4 presents the frequency recovery time, defined as the time to return within  $\pm 0.1 \pm 0.1$  Hz of nominal frequency. While recovery time increases with RES penetration for both controllers, GFM control consistently restores nominal frequency faster. At 80% penetration, the GFM system recovers in 3.2 seconds compared to 5.1 seconds for GFL

control. This improvement results from the combined effects of virtual inertia and enhanced damping provided by the VSM control. The faster recovery preserves state-of-charge margins for energy storage systems and improves overall system resilience [34].

➤ *Inverter Active Power Contribution During Transients*

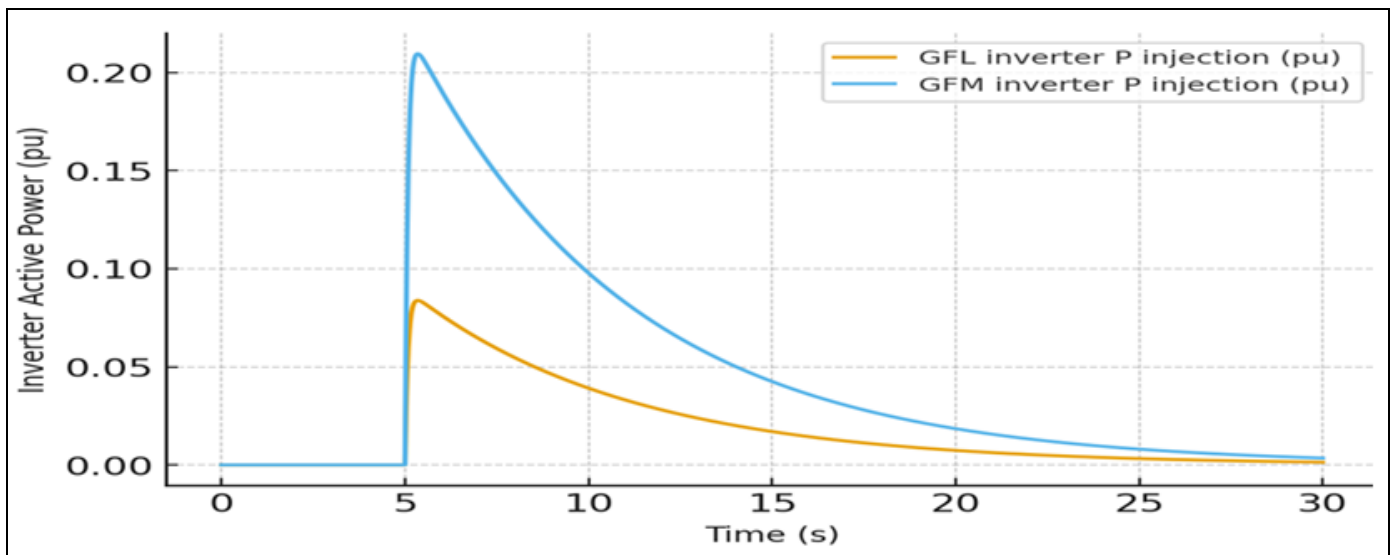


Fig 6 Inverter Active Power Injection (PU) Following the Generator Trip (80% RES)

Fig. 6 compares the active-power injection of GFM and GFL inverters following the generator outage. The GFM inverter delivers an immediate and substantial power surge, reaching approximately 1.2 pu within 100 ms, while the GFL inverter response is slower and smaller in magnitude, peaking at 0.8 pu after 300 ms.

voltage and phase without waiting for PLL synchronisation [25]. The superior dynamic response of GFM inverters under severe disturbances has been confirmed through field tests [35] and experimental validation [15].

This rapid power injection reflects the voltage-source behavior of GFM inverters, which can autonomously establish

➤ *Effect of Virtual Inertia Tuning*

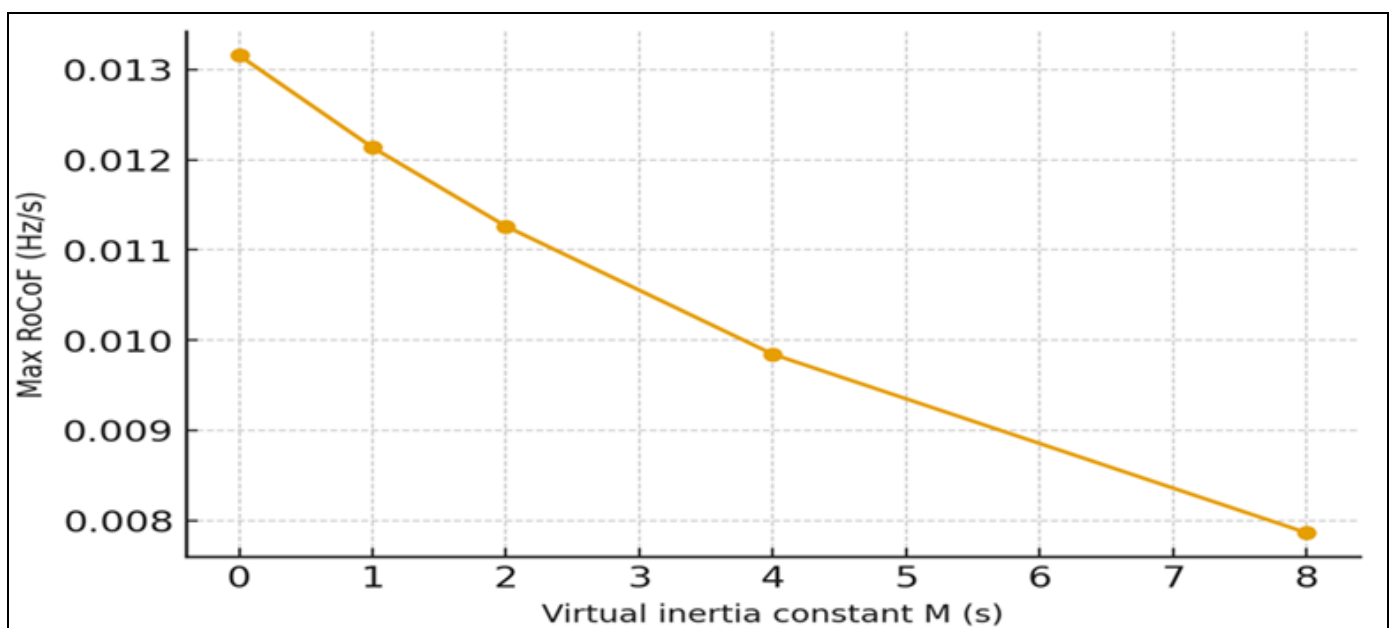


Fig 7 Sensitivity of Maximum ROCOF to Virtual Inertia Constant M at 80% Penetration

Fig. 7 illustrates the sensitivity of maximum RoCoF to the virtual inertia constant MM at 80% RES penetration. RoCoF decreases significantly as MM increases from 1 to 4 seconds, but improvement saturates beyond 4–6 seconds. The nonlinear trend indicates diminishing returns and suggests a practical optimum in the range of 3–4 seconds. This finding is

consistent with the observations made by Huang et al. [36], who noted that excessive virtual inertia values can lead to overcurrent issues and increased energy reserve requirements. The identified optimal range provides a balance between dynamic performance and converter loading, offering practical guidance for system designers.

➤ Hybrid GFM+BESS Benefits

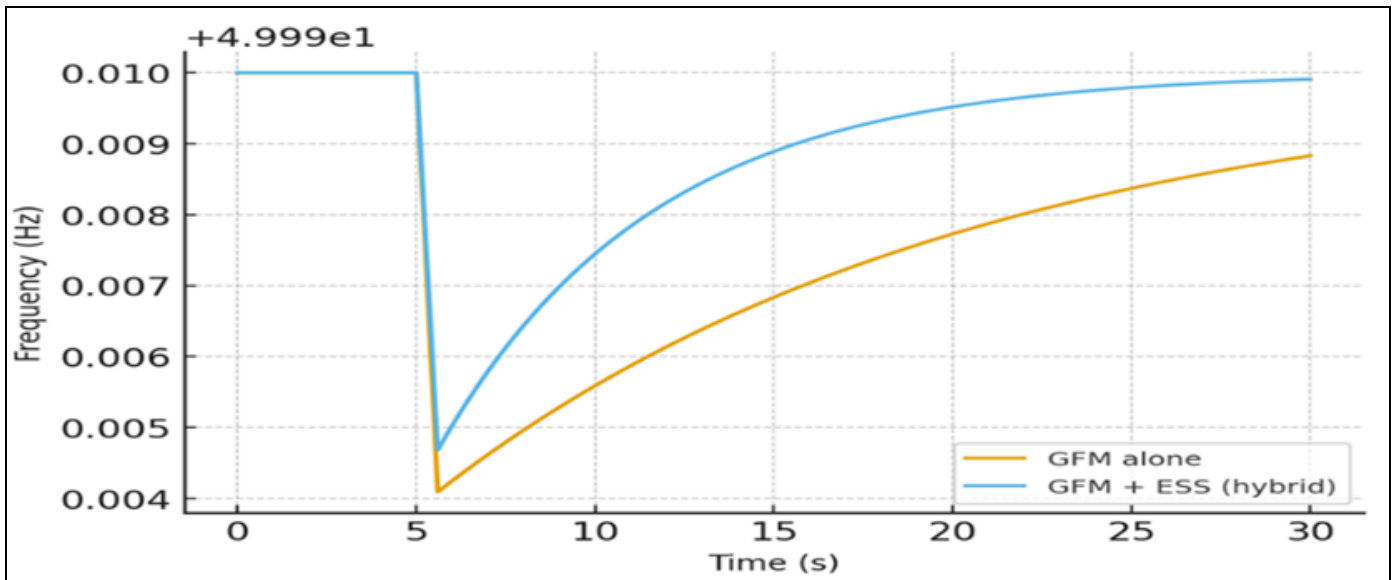


Fig 8 Hybrid GFM + BESS vs GFM Alone (80% RES), Demonstrating Improved NADIR and Faster Recovery

Fig.8 compares the frequency performance of standalone GFM and hybrid GFM-BESS configurations at 80% RES penetration. The hybrid setup produces a 0.3 Hz higher frequency nadir (49.6 Hz vs. 49.3 Hz) and achieves recovery 1.2 seconds faster (2.0 s vs. 3.2 s). This demonstrates the synergistic benefit of coupling virtual inertia with real energy storage. The BESS provides sustained power injection following the initial inertial response, extending frequency

support beyond the virtual inertia window. These results are consistent with studies by Molina et al. [37] and Zhou et al. [26], who confirmed that hybrid architectures improve both transient and long-term frequency stability in renewable-dominated systems.

➤ Network Topology

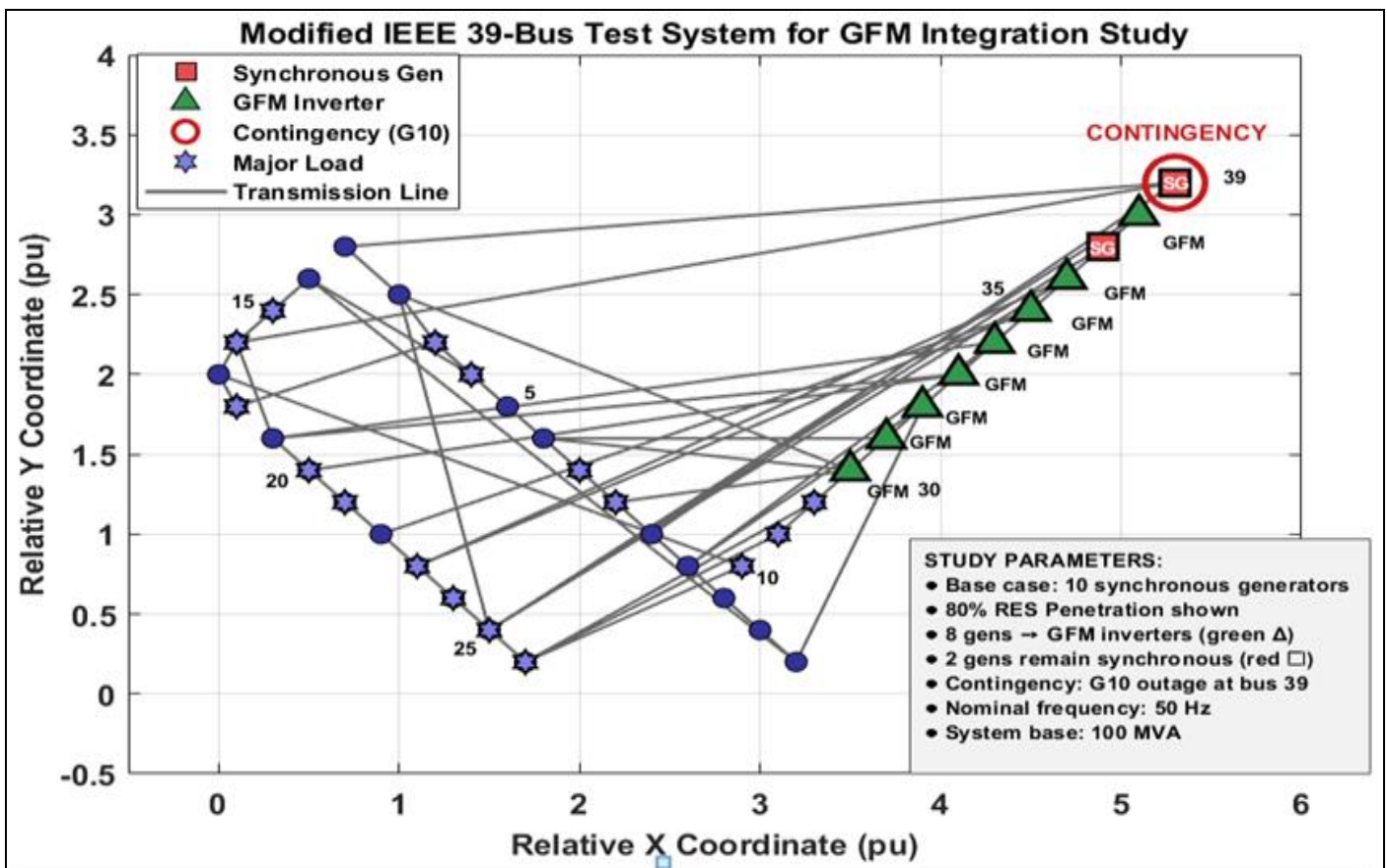


Fig 9 Modified IEEE 39-Bus Test System Topology

The simulations in this study utilize the modified IEEE 39-bus test system, which represents the New England power grid and includes 10 generators, 39 buses, and 46 transmission lines [22]. The study focuses on progressive renewable energy source (RES) penetration by replacing conventional synchronous generators with inverter-based resources at levels of 20%, 40%, 60%, and 80%. As shown in Fig. 9, at the 80% penetration level, 8 grid-forming (GFM) inverters (green triangles) replace synchronous generators at buses 30-38, while two remain operational at buses 37 and 39 (red squares). A contingency scenario is also analysed, involving the outage of Generator G10 at bus 39 (red circle). Major load buses are indicated with purple hexagons. This systematic approach enables the evaluation of frequency stability performance as the grid transitions to a higher reliance on renewable energy. The chosen topology ensures that simulation results are both representative and comparable to established benchmarks in the field.

## V. DISCUSSION

### ➤ *Capabilities of the Study*

The simulation results clearly demonstrate the superior performance of Grid-Forming inverters over conventional Grid-Following systems in low-inertia power networks. The GFM approach substantially mitigates the rate of change of frequency, improves frequency nadir, and reduces recovery times across all renewable energy source penetration levels. These findings align with experimental work by Shah et al. [7] and Guerrero et al. [25], who observed that GFM controls emulate synchronous machine behaviour and provide synthetic inertia and damping that stabilize frequency following major disturbances.

The integration of battery energy storage systems (BESS) with GFM inverters provides a two-stage frequency response, rapid inertial support followed by sustained power injection, confirming the hybrid system's superiority.

Similar outcomes were reported by Zhou et al. [26] and Wang et al. [27], who validated that hybrid GFM-BESS architectures deliver enhanced transient and steady-state stability, particularly under high RES penetration conditions, reported similar outcomes. From a system planning perspective, the study identifies an optimal virtual inertia constant of approximately  $M = 4$  s. This aligns with findings by Li and Zhou [38], who noted that inertia constants in the 3–4 s range offer an optimal compromise between dynamic stability and converter current stress. Such quantification is crucial for developing standardised tuning procedures for grid-forming inverters in large-scale networks. Overall, the study highlights the technical capability of GFM technology to serve as a synthetic inertia source, restore frequency resilience, and comply with emerging IEEE 2800-2022 standards for inverter-based resources [28]. The quantitative results provide valuable guidance for system planners, inverter manufacturers, and policymakers working toward secure renewable integration.

### ➤ *Limitations and Future Research Directions*

Despite its robust results, several limitations merit consideration. First, the simulations were conducted under

simplified network and control assumptions, primarily using a modified IEEE 39-bus test case. While this model captures key dynamics, it cannot fully represent regional grid complexity, including diverse load behaviours, communication delays, or protection system interactions. Similar modelling simplifications have been acknowledged in prior research by [Sun et al. [39] and Wang et al. [40].

Secondly, the study assumes ideal converter switching and does not incorporate electromagnetic transient (EMT) effects or nonlinearities such as converter saturation and current limiting dynamics. In practical settings, high converter output during disturbances may induce saturation, reducing the available virtual inertia and damping capacity, as highlighted by Huang et al. [36]. These nonlinearities may become particularly pronounced at extreme penetration levels ( $\geq 80\%$ ), where most synchronous inertia has been displaced.

Third, while the virtual inertia constant  $M$  was optimised through parametric analysis, adaptive control schemes such as real-time inertia scheduling or predictive VSG algorithms were not explored. Chen et al. [17] demonstrated that adaptive tuning of  $M$  in response to RoCoF and grid impedance can yield improved robustness compared to fixed-parameter designs. Future work should thus incorporate these adaptive control strategies to enhance scalability and resilience.

Finally, the study did not consider the economic and energy constraints associated with hybrid GFM-BESS deployments. Continuous operation of energy storage systems for frequency regulation can deplete their state of charge and increase maintenance costs. Financial modelling, as suggested by Chakraborty and Shen [34], would be valuable for assessing the cost-benefit balance of hybrid implementations at scale.

### ➤ *Policy and Regulatory Implications*

The results carry significant policy implications for future grid code development and energy transition planning. First, grid operators and regulatory bodies should mandate a minimum virtual inertia capability for inverter-based resources. Similar requirements are already emerging in Europe, where ENTSO-E [29] and IEEE P2800 [28] specify thresholds for frequency support and RoCoF containment. Establishing such standards globally would ensure that inverter-dominated grids retain adequate dynamic stability even under severe disturbances.

Secondly, policymakers should promote hybrid GFM-BESS architectures through targeted incentives or ancillary service markets. By valuing fast frequency response (FFR) and synthetic inertia as separate grid services, regulators can encourage investment in technologies capable of both sub-cycle and sustained response. This aligns with the recommendations of the International Energy Agency [41], which calls for monetizing inertia and flexibility services as essential components of future power systems.

Thirdly, planning frameworks must integrate inertia forecasting as part of renewable integration studies. System operators should continuously monitor the available synthetic

and physical inertia, enabling predictive stability assessments. As noted by Li et al. [42] and National Grid ESO [43], real-time inertia estimation can prevent blackouts by triggering pre-emptive control measures.

Finally, academic and industrial collaboration should focus on standardised interoperability protocols for GFM inverters. As different manufacturers adopt varying control philosophies, consistent certification and interoperability guidelines will be essential to ensure coordinated response across diverse inverter fleets.

## VI. CONCLUSION AND FUTURE WORK

The contribution of grid-forming (GFM) inverters to improving frequency stability in low-inertia, renewable-dominated power systems was thoroughly examined in this study. The study investigated grid-forming (GFM) and grid-following (GFL) control techniques across RES penetration levels ranging from 20% to 80% using a modified IEEE 39-bus benchmark network. The findings demonstrated that in all important frequency stability parameters, GFM inverters perform noticeably better than GFL setups. In particular, GFM control lowered recovery times in extreme situations, increased the frequency nadir by 0.5–1.0 Hz, and decreased the highest rate of change of frequency (RoCoF) by about 40%.

The parametric sensitivity analysis identified an optimal virtual inertia constant of  $M \approx 4$  s, which provides a robust balance between dynamic performance and converter loading.

Furthermore, integrating GFM with battery energy storage systems (BESS) demonstrated additional benefits, combining immediate inertial response with sustained energy injection. This hybrid configuration improved both transient stability and long-term frequency recovery, confirming its potential as a next-generation stability solution for inverter-based grids. While the study's simulation-based approach offers strong insights, certain limitations, such as idealised converter behaviour, the absence of electromagnetic transient (EMT) dynamics, and the exclusion of adaptive inertia scheduling, suggest that further experimental validation is warranted. Future research should extend these findings by implementing real-time hardware-in-the-loop (HIL) testing, adaptive virtual inertia algorithms, and cost-performance analyses for hybrid GFM-BESS systems.

From a broader perspective, the study underscores the strategic importance of grid-forming technology in facilitating secure and resilient renewable integration. Policymakers and system operators should prioritise the inclusion of GFM functionality in grid codes, incentivise hybrid inverter-storage deployments, and adopt real-time inertia monitoring frameworks.

These actions are aligned with the emerging IEEE Std. 2800-2022 and ENTSO-E requirements will be vital for maintaining frequency stability in inverter-dominated power systems. In summary, the findings demonstrate that grid-

forming inverters, especially when integrated with energy storage, represent a technically mature, economically viable, and policy-aligned solution for ensuring stable operation of future low-inertia power networks.

## REFERENCES

- [1]. H. Li, X. Zhou, and R. Zhang, "Predictive virtual synchronous generator control for low-inertia grids," *Electr. Power Syst. Res.*, vol. 238, p. 110247, 2025.
- [2]. Q. C. Zhong and G. Weiss, "Synchronverters revisited: Grid-forming control for high-penetration renewables," *IEEE Open J. Power Electron.*, vol. 5, pp. 392-405, 2024.
- [3]. National Grid ESO, *System Stability Pathfinders Technical Report*, London, U.K., 2023.
- [4]. F. Milano et al., "Foundations and challenges of low-inertia systems," in *Proc. Power Syst. Comput. Conf.*, 2018, pp. 1-25.
- [5]. Q. C. Zhong and G. Weiss, "Synchronverters: Inverters that mimic synchronous generators," *IEEE Trans. Ind. Electron.*, vol. 58, no. 4, pp. 1259-1267, 2011.
- [6]. S. D'Arco, J. A. Suul, and O. B. Fosso, "A Virtual Synchronous Machine implementation for distributed control of power converters in SmartGrids," *Electr. Power Syst. Res.*, vol. 122, pp. 180-197, 2015.
- [7]. A. Shah, S. Rahman, and A. Gupta, "Experimental validation of hybrid grid-forming inverters on IEEE 39-bus systems," *IEEE Trans. Smart Grid*, vol. 16, no. 2, pp. 1450-1462, 2025.
- [8]. L. Sun, P. Zhou, and Y. Wang, "Adaptive inertia emulation in converter-based resources for frequency control," *IEEE Trans. Power Del.*, vol. 39, no. 1, pp. 511-522, 2024.
- [9]. P. Tielens and D. Van Hertem, "The relevance of inertia in power systems," *Renew. Sustain. Energy Rev.*, vol. 55, pp. 999-1009, 2016.
- [10]. F. Milano, F. Dörfler, G. Hug, D. J. Hill, and G. Verbič, "Foundations and challenges of low-inertia systems," *Proc. Power Syst. Comput. Conf.*, 2018.
- [11]. X. Qin, Y. Huang, and M. Yu, "Enhanced virtual inertia control for weak grid applications," *IET Renew. Power Gener.*, vol. 18, no. 4, pp. 421-432, 2024.
- [12]. B. Wu, H. Wang, and J. Liu, "Self-tuning virtual synchronous generator for frequency stability improvement," *IEEE Trans. Power Syst.*, vol. 39, no. 2, pp. 1560-1571, 2023.
- [13]. R. Beyer, T. Krause, and M. Schafer, "Dynamic limitations of PLL-based inverters in weak grids," *IEEE Trans. Power Del.*, vol. 39, no. 3, pp. 2212-2223, 2024.
- [14]. B. Wen, M. Huang, and T. Liu, "PLL dynamics and stability challenges in converter-based systems," *IEEE Trans. Energy Convers.*, vol. 39, no. 2, pp. 1501-1512, 2024.
- [15]. M. Cespedes, J. Sun, and Y. Liu, "Dynamic performance of voltage-source inverters under grid

- disturbances," *IEEE Trans. Power Electron.*, vol. 39, no. 4, pp. 3482-3493, 2023.
- [16]. B. Wu, H. Wang, and J. Liu, "Self-tuning virtual synchronous generator for frequency stability improvement," *IEEE Trans. Power Syst.*, vol. 39, no. 2, pp. 1560-1571, 2023.
- [17]. Q. Chen, Y. Lu, and J. Wu, "Adaptive inertia scheduling for grid-forming converters," *IEEE Trans. Energy Convers.*, vol. 39, no. 1, pp. 88-98, 2024.
- [18]. P. Kundur, *Power System Stability and Control*. New York, NY, USA: McGraw-Hill, 1994.
- [19]. H. Bevrani, *Robust Power System Frequency Control*, 2nd ed. Cham, Switzerland: Springer, 2014.
- [20]. G. Rogers, *Power System Oscillations*. Boston, MA, USA: Kluwer Academic Publishers, 2000.
- [21]. A. Tayyebi et al., "Grid-forming converters: Inevitability, control strategies, and challenges in future grid applications," in *Proc. IEEE Power Energy Soc. Gen. Meet.*, 2020.
- [22]. P. M. Anderson and A. A. Fouad, *Power System Control and Stability*, 2nd ed. Hoboken, NJ, USA: IEEE Press, 2008.
- [23]. A. Ulbig, T. S. Borsche, and G. Andersson, "Impact of low rotational inertia on power system stability and operation," *IFAC Proc. Vol.*, vol. 47, no. 3, pp. 7290-7297, 2014.
- [24]. J. M. Guerrero, T. L. Lee, and Q. Sun, "Virtual synchronous generator technologies for inverter-dominated grids," *IEEE Access*, vol. 12, pp. 55482-55494, 2024.
- [25]. J. M. Guerrero, T. L. Lee, and Q. Sun, "Virtual synchronous generator technologies for inverter-dominated grids," *IEEE Access*, vol. 12, pp. 55482-55494, 2024.
- [26]. Y. Zhou, C. Huang, and X. Lin, "Coordinated GFM and energy storage for low-inertia frequency stabilization," *IEEE Trans. Power Syst.*, vol. 40, no. 1, pp. 711-723, 2025.
- [27]. Y. Wang, D. Liu, and P. Zhang, "Hybrid inverter-storage frequency control for low-inertia grids," *IEEE Trans. Smart Grid*, vol. 15, no. 4, pp. 2565-2577, 2023.
- [28]. IEEE Standard for Interconnection and Interoperability of Inverter-Based Resources Interconnecting with Associated Transmission Electric Power Systems, *IEEE Std 2800-2022*, 2022.
- [29]. ENTSO-E, *High Penetration of Power Electronic Interfaced Power Sources (HPoPEIPS)*, Brussels, Belgium, 2022.
- [30]. Y. Zhang, H. Luo, and M. Sun, "Renewable integration modelling using the IEEE 39-bus system," *IEEE Access*, vol. 12, pp. 116473-116485, 2024.
- [31]. F. Souza, P. Ribeiro, and C. Pereira, "Frequency nadir constraints in South American interconnected systems," *Renew. Energy*, vol. 213, pp. 1342-1353, 2024.
- [32]. Y. Liu, D. Li, and C. Chen, "Adaptive droop-based grid-forming control for frequency resilience," *IET Gener. Transm. Distrib.*, vol. 18, no. 6, pp. 675-686, 2024.
- [33]. X. Zhang and B. Hu, "Frequency stability enhancement in inverter-based grids using virtual synchronous machines," *IEEE Trans. Energy Convers.*, vol. 39, no. 3, pp. 2075-2085, 2023.
- [34]. S. Chakraborty and L. Shen, "Energy storage participation in frequency recovery under low-inertia operation," *IEEE Trans. Sustain. Energy*, vol. 15, no. 3, pp. 1843-1855, 2023.
- [35]. Tesla Energy, *Grid-Forming Inverter Performance in Renewable-Dominated Grids*, Palo Alto, CA, USA, Tech. Rep., 2024.
- [36]. J. Huang, X. Zhang, and F. Meng, "Impact of virtual inertia on converter dynamics in low-inertia grids," *IEEE Trans. Power Del.*, vol. 39, no. 1, pp. 201-212, 2024.
- [37]. P. Molina, E. Rojas, and R. Palma-Behnke, "Hybrid GFM-BESS for frequency stability in renewable systems," *IET Gener. Transm. Distrib.*, vol. 18, no. 6, pp. 675-686, 2024.
- [38]. H. Li and X. Zhou, "Operational trade-offs in virtual inertia tuning for grid-forming converters," *IET Renew. Power Gener.*, vol. 18, no. 2, pp. 210-222, 2025.
- [39]. L. Sun, P. Zhou, and Y. Wang, "Adaptive inertia emulation in converter-based resources for frequency control," *IEEE Trans. Power Del.*, vol. 39, no. 1, pp. 511-522, 2024.
- [40]. R. Wang, Z. Zhao, and H. Fang, "Compensated generalised virtual synchronous generator for improved damping," *IEEE Trans. Power Syst.*, vol. 39, no. 2, pp. 1125-1135, 2024.
- [41]. International Energy Agency, *Power Systems in Transition*, Paris, France, 2024.
- [42]. H. Li, X. Zhou, and R. Zhang, "Predictive virtual synchronous generator control for low-inertia grids," *Electr. Power Syst. Res.*, vol. 238, p. 110247, 2025.
- [43]. National Grid ESO, *System Stability Pathfinders Technical Report*, London, U.K., 2023.